Driving atoms with light of arbitrary statistics

C. W. Gardiner and A. S. Parkins
Physics Department, University of Waikato, Hamilton, New Zealand
(Received 18 October 1993)

The coupled-systems approach of Gardiner [Phys. Rev. Lett. **70**, 2269 (1993)] and Carmichael [Phys. Rev. Lett. **70**, 2273 (1993)] is used to study the effects of driving systems by a variety of kinds of nonclassical light, namely, squeezed light, two-mode squeezed light, antibunched light from a two-level atom driven by either coherent light or finite-bandwidth thermal light, and the light from a single atom in a very-high-Q cavity. The method is shown to be very efficient and complete. It is also shown that the photon-counting properties of light from an atom driven by antibunched light are not determined solely by the antibunching of the driving light.

PACS number(s): 42.50.Dv, 42.50.Lc, 42.50.Ct

I. INTRODUCTION

The development of the input-output formalism by Gardiner and Collett [1], based on the "quantum network theory" of Yurke and Denker [2] gave rise to the possibility of a kind of "modular quantum optics," in which nonclassical light beams could be generated and then used as inputs to other quantum systems. Early work by Kolobov and Sokolov [3] gave an indication of how this might be done, and more recently Gardiner [4] and Carmichael [5] gave what amounted to the same formalism, though in each case with a very different derivation.

Until recently there has been no need for such a formalism, since reliable sources of nonclassical light with useable intensity have not been generally available. The situation is, however, now changing, with many groups around the world producing squeezed, antibunched, and sub-Poissonian light beams [6–8].

The aim of this paper is to consolidate the work of Refs. [3–5] and to extend it to include the possibilities of

(i) multiple input and output into each system;

(ii) longer (possibly branched) chains of sytems, each driving the next;

(iii) arbitrary quantum white noise inputs into the atoms.

After extending the formalism, we use it in a number of applications. In Sec. III we consider the situation in which the first system is describable by harmonic oscillator operators, which may be driven by various Gaussian inputs. The two particular systems we consider are an empty cavity driven by a broadband thermal field, and a degenerate parametric amplifier. The outputs from these are, respectively, finite-bandwidth thermal light and squeezed light, which then drive the second system. We show how, by using the positive P representation, we can derive the formalism used by Parkins and Gardiner [9] and by Ritsch and Zoller [10] in considering the inhibition of atomic phase decays by squeezed light.

Section IV concentrates on numerical results for atomic systems driven by squeezed light. The advantage of the coupled systems approach here arises from the possibility of truncating the harmonic oscillator systems to only a few levels—no more than ten were found necessary—and thus being able to solve the master equation by direct numerical integration in spaces of perhaps a few hundred dimensions. This is very much more efficient than previous numerical methods, particularly those based on stochastic simulations. We present results for the inhibition of atomic phase decays in a two-level atom driven by squeezed light, and for two-photon absorption by a three-level system driven by correlated photons from a nondegenerate parametric amplifier. The first of these should be considered as a demonstration of the method, while the second is in principle a much more thorough treatment than those used previously, which have depended on either the approximation of infinite bandwidth of the squeezed light or on weak field approximations. The results—a linear dependence of the two-photon absorption rate on the intensity of the incoming field (rather than the quadratic dependence expected for uncorrelated inputs)—are much the same as previously computed, but this is largely because we have investigated only the weak-driving-field limit.

In Sec. V we give a treatment of a two-level atom driven by the antibunched light produced by another driven two-level atom. This is an extension of earlier work [4]. In this paper, we show that we can drive the first atom either with coherent light, or with finite-bandwidth thermal light, and get (by appropriate choices of parameters) the same output intensity and intensity correlation function $g^{(2)}(t)$, though different spectral and other properties. The results of driving the second atom with these two kinds of light—which are identically antibunched—are significantly different from each other. We obtain the same qualitative results, that is, the output beams from the two atoms are antibunched and anticorrelated with each other, but the quantitative difference is quite significant.

In Sec. VI we consider the driving of a two-level atom with the light produced by a system composed of a two-level atom and a very-high-Q cavity. This light has a number of rather nonclassical features. The results are interesting and rather intricate. We find a number of nonclassical effects, and in particular, we can see how to

produce light with antibunching extending over a rather longer time interval than would have been expected.

II. COUPLING EQUATIONS

The basic idea is very simple. We consider a quantum system which can be decomposed into two subsystems. Using the notation of Refs. [1, 11], a driving field $b_{\rm in}(1,t)$ drives the first system, and gives rise to an output $b_{\rm out}(1,t)$ which, after a propagation delay τ, becomes the input field $b_{\rm in}(2,t)$ to the second system: let a_1, a_2 be operators for the two systems, and let $H_{\rm sys}$ be the sum of their otherwise independent system Hamiltonians. The situation is illustrated in Fig.1. The quantum Langevin equations for these are

$$\dot{a}_1 = -\frac{i}{\hbar}[a_1, H_{\rm sys}] - [a_1, c_1^\dagger]\left\{\frac{\gamma_1}{2}c_1 + \sqrt{\gamma_1}b_{\rm in}(1,t)\right\} + \left\{\frac{\gamma_1}{2}c_1^\dagger + \sqrt{\gamma_1}b_{\rm in}^\dagger(1,t)\right\}[a_1, c_1], \quad (1)$$

$$\dot{a}_2 = -\frac{i}{\hbar}[a_2, H_{\rm sys}] - [a_2, c_2^\dagger]\left\{\frac{\gamma_2}{2}c_2 + \sqrt{\gamma_2}b_{\rm in}(2,t)\right\} + \left\{\frac{\gamma_2}{2}c_2^\dagger + \sqrt{\gamma_2}b_{\rm in}^\dagger(2,t)\right\}[a_2, c_2]. \quad (2)$$

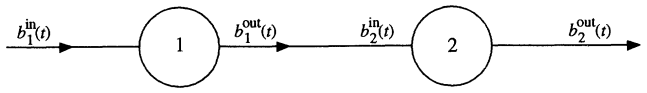

FIG. 1. Schematic diagram indicating how system 2 is driven by the output from system 1.

The output field from the first system is given by

$$b_{\rm out}(1,t) = b_{\rm in}(1,t) + \sqrt{\gamma_1}c_1(t). \quad (3)$$

If it takes a time τ for light to travel from system 1 to system 2, then we can get the effect of feeding the output of system 1 into the input of system 2 by writing

$$b_{\rm in}(2,t) = b_{\rm out}(1,t-\tau) = b_{\rm in}(1,t-\tau) + \sqrt{\gamma_1}c_1(t-\tau). \quad (4)$$

If now a is an operator from either of the systems, the resulting two quantum Langevin equations can be written as one equation for a [using the abbreviated notation $b_{\rm in}(1,t) \to b_{\rm in}(t)$]:

$$\dot{a} = -\frac{i}{\hbar}[a, H_{\rm sys}] - [a, c_1^\dagger]\left\{\frac{\gamma_1}{2}c_1 + \sqrt{\gamma_1}b_{\rm in}(t)\right\} + \left\{\frac{\gamma_1}{2}c_1^\dagger + \sqrt{\gamma_1}b_{\rm in}^\dagger(t)\right\}[a, c_1]$$
$$-[a, c_2^\dagger]\left\{\frac{\gamma_2}{2}c_2 + \sqrt{\gamma_1\gamma_2}c_1(t-\tau) + \sqrt{\gamma_2}b_{\rm in}(t-\tau)\right\} + \left\{\frac{\gamma_2}{2}c_2^\dagger + \sqrt{\gamma_1\gamma_2}c_1^\dagger(t-\tau) + \sqrt{\gamma_2}b_{\rm in}^\dagger(t-\tau)\right\}[a, c_2]. \quad (5)$$

These equations are deliberately called quantum *Langevin* equations (rather than quantum stochastic differential equations) because the statistics of the input fields is not specified—they are thus valid for arbitrary statistics of the input fields.

In developing these equations it has been required that the output from the first atom can be connected to the input of the second atom without there being a corresponding connection from the second atom back into the first. Experimentally, this is routinely achieved by appropriate isolation techniques, and it is possible to write such a one-way coupling in terms of a Hamiltonian, as has already been shown in Ref. [4]—in fact (5) is derived from a Hamiltonian directly in Ref. [4].

The major technical difficulty is the fact that operators at the two times t and $t-\tau$ both turn up. Because we are considering only the case in which the driving is one way, it is clear that τ may be chosen arbitrarily—its only effect is to shift the origin of the time axis for the second atom.

To see this explicitly, note that Eq. (5) takes on different forms depending on whether a is an operator from the first atom or the second. To put these in the simplest form we proceed as follows.

(i) Define an advanced operator $\hat{a}(t) \equiv a(t+\tau)$.

(ii) Note that we can write $H_{\rm sys} = H_1 + H_2$, where the two parts are operators only in the first and second spaces, respectively.

(iii) If a_1, a_2 represent arbitrary operators in the first and second systems, respectively, Eq. (5) gives the two equations

$$\frac{da_1}{dt} = -\frac{i}{\hbar}[a_1, H_1] - [a_1, c_1^\dagger]\left\{\frac{\gamma_1}{2}c_1 + \sqrt{\gamma_1}b_{\rm in}(t)\right\} + \left\{\frac{\gamma_1}{2}c_1^\dagger + \sqrt{\gamma_1}b_{\rm in}^\dagger(t)\right\}[a_1, c_1], \quad (6)$$

$$\frac{d\hat{a}_2}{dt} = -\frac{i}{\hbar}[\hat{a}_2, \hat{H}_1] - [\hat{a}_2, \hat{c}_2^\dagger]\left\{\frac{\gamma_2}{2}\hat{c}_2 + \sqrt{\gamma_1\gamma_2}c_1 + \sqrt{\gamma_2}b_{\rm in}(t)\right\} + \left\{\frac{\gamma_2}{2}\hat{c}_2^\dagger + \sqrt{\gamma_1\gamma_2}c_1^\dagger + \sqrt{\gamma_2}b_{\rm in}^\dagger(t)\right\}[\hat{a}_2, \hat{c}_2]. \quad (7)$$

There is now only one time in the resulting equations, and the solutions for these equations provide all the information required to describe the system, since they are valid for arbitrary operators in acting on one space or the other, in terms of which any other operator can also be written. The same result is obtained simply by setting $\tau = 0$ in (5), and omitting the rather cumbersome $\hat{a}_2$ notation, and this is what we shall do from now on. Notice, however, that the procedure works only because of the explicit one-way nature of the interaction between the two systems.

A. Conversion to quantum Ito equations and derivation of the master equation

Although the quantum Langevin equations give an elegant description of the physics involved, the equivalent

master equation will provide a much more tractable way of treating the problems numerically. To this end we want to convert the quantum Langevin equations into quantum Ito stochastic differential equations, from which an appropriate master equation can be derived, using standard methods [1, 11].

If we consider the general case in which the input field can be written in terms of a coherent part and a quantum white noise part

$$b_{\rm in}(t)\,dt = dB(t) + \mathcal{E}(t)\,dt \tag{8}$$

with

$$[dB(t)]^2 = [dB^\dagger(t)]^2 = 0, \tag{9}$$

$$dB(t)dB^\dagger(t) = (\bar{N}+1)dt, \tag{10}$$

$$[dB(t)]^\dagger dB(t) = \bar{N}\,dt, \tag{11}$$

then the equivalent Ito white noise quantum stochastic differential equation is

$$\begin{aligned} da = &-\frac{i}{\hbar}[a, H_{\rm sys}]dt - [a, c_1^\dagger]\left\{\frac{\gamma_1}{2}c_1 + \sqrt{\gamma_1}\mathcal{E}_{\rm in}(t)\right\}dt + \left\{\frac{\gamma_1}{2}c_1^\dagger + \sqrt{\gamma_1}\mathcal{E}_{\rm in}^*(t)\right\}[a, c_1]dt \\ &-[a, c_2^\dagger]\left\{\frac{\gamma_2}{2}c_2 + \sqrt{\gamma_1\gamma_2}c_1 + \sqrt{\gamma_2}\mathcal{E}_{\rm in}(t)\right\}dt + \left\{\frac{\gamma_2}{2}c_2^\dagger + \sqrt{\gamma_1\gamma_2}c_1^\dagger + \sqrt{\gamma_2}\mathcal{E}_{\rm in}^*(t)\right\}[a, c_2]dt \\ &-\frac{\bar{N}}{2}[[a, \sqrt{\gamma_1}c_1^\dagger + \sqrt{\gamma_2}c_2^\dagger], \sqrt{\gamma_1}c_1 + \sqrt{\gamma_2}c_2]dt - \frac{\bar{N}}{2}[\sqrt{\gamma_1}c_1^\dagger + \sqrt{\gamma_2}c_2^\dagger, [\sqrt{\gamma_1}c_1 + \sqrt{\gamma_2}c_2, a]]dt \\ &-\sqrt{\gamma_1}[a, c_1^\dagger]dB(t) + \sqrt{\gamma_1}dB^\dagger(t)[a, c_1] - \sqrt{\gamma_2}[a, c_2^\dagger]dB(t) + \sqrt{\gamma_2}dB^\dagger(t)[a, c_2]. \end{aligned} \tag{12}$$

From this it follows that a master equation can be derived for the density operator $\rho(t)$ by the usual technique [1, 11] of setting $\langle da(t)\rho\rangle \equiv \langle da\rho(t)\rangle$, and this master equation takes the form

$$\begin{aligned} \frac{d\rho}{dt} = &\frac{i}{\hbar}[\rho, H_{\rm sys}] + \frac{\gamma_1}{2}\{2c_1\rho c_1^\dagger - \rho c_1^\dagger c_1 - c_1^\dagger c_1\rho\} + \frac{\gamma_2}{2}\{2c_2\rho c_2^\dagger - \rho c_2^\dagger c_2 - c_2^\dagger c_2\rho\} \\ &-\sqrt{\gamma_1\gamma_2}\{[c_2^\dagger, c_1\rho] + [\rho c_1^\dagger, c_2]\} + \frac{\bar{N}}{2}[[\sqrt{\gamma_1}c_1 + \sqrt{\gamma_2}c_2, \rho], \sqrt{\gamma_1}c_1^\dagger + \sqrt{\gamma_2}c_2^\dagger] \\ &+\frac{\bar{N}}{2}[[\sqrt{\gamma_1}c_1^\dagger + \sqrt{\gamma_2}c_2^\dagger, \rho], \sqrt{\gamma_1}c_1 + \sqrt{\gamma_2}c_2] - [\mathcal{E}_{\rm in}(t)(\sqrt{\gamma_1}c_1^\dagger + \sqrt{\gamma_2}c_2^\dagger) - \mathcal{E}_{\rm in}^*(t)(\sqrt{\gamma_1}c_1 + \sqrt{\gamma_2}c_2), \rho]. \end{aligned} \tag{13}$$

B. Imperfect coupling

In the previous section we considered the case in which all of the output of the first system was used as the input to the second system. This is usually not realistic, since

(i) there must be some losses in transmission.

(ii) We may not wish to couple perfectly from the first to the second system.

For example, by (3), any coherent component of $b_{\rm in}(t)$ will appear in $b_{\rm out}(t)$, and hence in $b_{\rm in}(t)$. We may wish to do this, but we may also wish to investigate the effect of illuminating the second system with only the *fluorescent* light [represented in (3) by $\sqrt{\gamma_1}c_1(t)$] from the first system.

This can be done by considering the coupling of the first system to two channels with the same kind of coupling (though of different strength), as illustrated in Fig. 2. We thus modify the quantum Langevin equation (1) by setting

$$b_{\rm in}(t) = \sqrt{\epsilon_1}\,f_{\rm in}(t) + \sqrt{(1-\epsilon_1)}\,g_{\rm in}(t) \tag{14}$$

with $0 \le \epsilon_1 \le 1$. Here $f_{\rm in}(t)$ and $g_{\rm in}(t)$ together make up all the coupling available to radiated modes, so that the total damping constant is simply γ_1. There are then two output fields given by

$$f_{\rm out}(t) = f_{\rm in}(t) + \sqrt{\epsilon_1\gamma_1}\,c_1(t), \tag{15}$$

$$g_{\rm out}(t) = g_{\rm in}(t) + \sqrt{(1-\epsilon_1)\gamma_1}\,c_1(t). \tag{16}$$

If we now consider a situation in which we drive the system with a coherent field in the $f_{\rm in}$ channel, it is clear

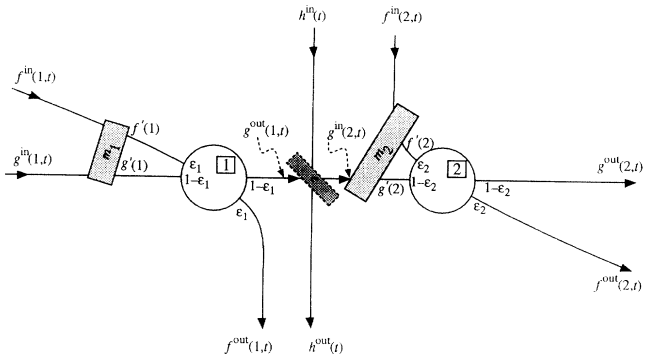

FIG. 2. Arrangements required to account for imperfect coupling. The systems are considered to have two input-output channels. The corresponding fields are coupled with strengths $\sqrt{\epsilon_i}$, $\sqrt{1-\epsilon_i}$, so that the *total* coupling is the same independent of ϵ_i. To account for the possibility that the input channel to the second system may not match perfectly with an output channel from the first system, a *unitary mixer* m_1 is inserted between the physical inputs, and those corresponding to the required outputs. The same is done for the second system. The beam splitter e is necessary to account for the fact the light in the relevant output channel may not all be fed into the relevant input channel in the second system.

that in the $g_{\rm out}$ channel we will see no component of the incoming driving field. Physically, we could consider the case where $f_{\rm in}$ represents a laser beam (almost a plane wave) while $g_{\rm out}$ is an outgoing electric dipole wave, observed away from the direction of the laser beam.

In coupling to the next system we must consider that some proportion of $g_{\rm out}$ will be lost in transmission. This can be modeled by inserting a beam splitter in the channel $g_{\rm out}$, so that we have

$$g_{\rm in}(2,t) = \sqrt{e_1}\, g_{\rm out}(1,t) + \sqrt{1-e_1}\, h_{\rm in}(t) \tag{17}$$

$$= \sqrt{e_1(1-\epsilon_1)\gamma_1}\, c_1(t) + \sqrt{e_1}\, g_{\rm in}(1,t) + \sqrt{1-e_1}\, h_{\rm in}(t), \tag{18}$$

where $h_{\rm in}(t)$ represents a vacuum field. The total field then enters the second system, with its complementary field $f_{\rm in}(2,t)$. Using (17) and (18), we find the quantum Langevin equation

$$\dot{a} = -\frac{i}{\hbar}[a, H_{\rm sys}] - \left([a, c_1^\dagger]\left\{\frac{\gamma_1}{2}c_1 + \sqrt{\gamma_1\epsilon_1}\, f_{\rm in}(1,t) + \sqrt{\gamma_1(1-\epsilon_1)}\, g_{\rm in}(1,t)\right\} + \text{conjugate}\right)$$
$$-\left([a, c_2^\dagger]\left\{\frac{\gamma_2}{2}c_2 + \sqrt{\gamma_2\epsilon_2}\, f_{\rm in}(2,t) + \sqrt{\gamma_2(1-\epsilon_2)}\left[\sqrt{\gamma_1 e_1(1-\epsilon_1)}c_1(t-\tau)\right.\right.\right.$$
$$\left.\left.\left. + \sqrt{e_1}\, g_{\rm in}(1,t-\tau) + \sqrt{1-e_1}\, h_{\rm in}(t)\right]\right\} + \text{conjugate}\right). \tag{19}$$

In this equation, the term "conjugate" means that one should take the Hermitian conjugate of everything except a.

Master equation

In the case that $g_{\rm in}(1,t)$, $h_{\rm in}(t)$, and $f_{\rm in}(2,t)$ represent the vacuum, and we have a coherent driving field in the $f_{\rm in}$ channel of the first system, which we represent by

$$f_{\rm in}(1,t) = E(t) + f_{\rm in}^0(t), \tag{20}$$

where $f_{\rm in}^0(t)$ is a vacuum field, we can derive the master equation

$$\frac{\partial\rho}{\partial t} = \frac{i}{\hbar}[\rho, H_{\rm sys}] + \frac{\gamma_1}{2}\left\{2c_1\rho c_1^\dagger - \rho c_1^\dagger c_1 - c_1^\dagger c_1\rho\right\} + \frac{\gamma_2}{2}\left\{2c_2\rho c_2^\dagger - \rho c_2^\dagger c_2 - c_2^\dagger c_2\rho\right\}$$
$$-\sqrt{e_1\gamma_1\gamma_2(1-\epsilon_1)(1-\epsilon_2)}\{[c_2^\dagger, c_1\rho] + [\rho c_1^\dagger, c_2]\} - \sqrt{\gamma_1\epsilon_1}[E(t)c_1^\dagger + E^*(t)c_1, \rho]. \tag{21}$$

There is the further possibility that $g_{\rm out}$ and $f_{\rm out}$ may not correspond exactly to the $g_{\rm in}$ and $f_{\rm in}$. For example, a fraction of the coherent field in $f_{\rm in}(1,t)$ [see (20)] may be seen in $g_{\rm out}(1,t)$ due to some misalignment. This is best dealt with by putting a unitary mixer between $f_{\rm in}, g_{\rm in}$ and the system, so that the fields which correspond to $g_{\rm out}, f_{\rm out}$ are in fact

$$g'_{\rm in}(1,t) = \sqrt{m_1}\, g_{\rm in}(1,t) + \sqrt{1-m_1}\, f_{\rm in}(1,t), \tag{22}$$

$$f'_{\rm in}(1,t) = \sqrt{m_1}\, f_{\rm in}(1,t) - \sqrt{1-m_1}\, g_{\rm in}(1,t), \tag{23}$$

where $0 \le m_1 \le 1$ is a mixing parameter. (For simplicity we have adjusted arbitrary phases so that no complex coefficients are necessary.)

A similar thing can happen at the input to the second system. From all of these we get the master equation

$$\frac{\partial\rho}{\partial t} = \frac{i}{\hbar}[\rho, H_{\rm sys}] + \frac{\gamma_1}{2}\{2c_1\rho c_1^\dagger - \rho c_1^\dagger c_1 - c_1^\dagger c_1\rho\} + \frac{\gamma_2}{2}\{2c_2\rho c_2^\dagger - \rho c_2^\dagger c_2 - c_2^\dagger c_2\rho\}$$
$$-\sqrt{e_1\epsilon_1\gamma_1\gamma_2}\{\sqrt{m_2\epsilon_2} + \sqrt{(1-m_2)(1-\epsilon_2)}\}\{[c_2^\dagger, c_1\rho] + [\rho c_1^\dagger, c_2]\}$$
$$-\sqrt{\gamma_1}\{\sqrt{m_1\epsilon_1} + \sqrt{(1-m_1)(1-\epsilon_1)}\}[E(t)c_1^\dagger + E^*(t)c_1, \rho]$$
$$-\sqrt{\gamma_2 e_1(1-m_1)}\{\sqrt{m_2\epsilon_2} + \sqrt{(1-m_2)(1-\epsilon_2)}\}[E(t)c_2^\dagger + E^*(t)c_2, \rho]. \tag{24}$$

This equation represents the most general combination of mismatching and inefficient coupling for two coupled systems. For the purposes of solving this master equation, the mixing parameter m_2 is really an unnecessary complication, but in the case of several cascaded systems, it is essential.

III. HARMONIC OSCILLATOR SYSTEMS

In a series of papers, Parkins and Gardiner [9] and Ritsch and Zoller [10] considered the problem of the driving of a two-level atom with finite-bandwidth squeezed light, and developed numerical techniques based on either

stochastic simulations or on eigenfunction expansions for the Fokker-Planck equation to treat this kind of problem numerically. In this section we will show how the coupled-systems approach can provide a very much more efficient way of treating this and related problems. The idea is to use for the first system a model of a degenerate parametric oscillator, which is arguably the most favored source of squeezed light at present [8]. The methods of the previous section then produce a coupled master equation description, which we can show is exactly equivalent to the methods used by the above authors. However, it proves practicable to solve these equations numerically by truncating the infinite dimensional space of the harmonic oscillator operators used for the parametric oscillator to quite a small size, usually no more than ten dimensional matrices are sufficient for degrees of squeezing up to approximately 90%.

A. Driving by thermal light

Let us first consider a situation in which the first system is a thermally excited cavity, which yields a thermal light beam. This may be represented by a harmonic oscillator, with two inputs and outputs. One of the inputs is coupled to a finite temperature source of quantum white noise, and its corresponding output is not coupled to anything. The other input receives a vacuum, and its corresponding output drives the second system. The system may thus be represented by

$c_1, c_1^\dagger a, a^\dagger$; harmonic oscillator operators

$f_{\rm in}(1,t) \rightarrow$ quantum white noise, such that

$$\langle f_{\rm in}^\dagger(1,t) f_{\rm in}(1,t')\rangle = \bar{N}_0 \delta(t-t') \quad (25)$$

$g_{\rm in}(1,t) \rightarrow$ vacuum.

The first system can be thought of as a two-sided cavity, as in Fig. 3, and the master equation which arises from (21) becomes

$$\begin{aligned}\frac{\partial \rho}{\partial t} = \frac{i}{\hbar}[\rho, H_{\rm sys}] + \frac{\gamma_1}{2}\Big\{ &(\bar{N}+1)\{2a\rho a^\dagger - \rho a^\dagger a - a^\dagger a\rho\} \\ &+\bar{N}\{2a^\dagger \rho a - \rho a a^\dagger - a a^\dagger \rho\} \\ &+\frac{\gamma_2}{2}\{2c_2\rho c_2^\dagger - \rho c_2^\dagger c_2 - c_2^\dagger c_2 \rho\} \\ &-\sqrt{\eta\gamma_1\gamma_2}\{[c_2^\dagger, a\rho] + [\rho a^\dagger, c_2]\}\Big\} \end{aligned} \quad (26)$$

where, for brevity,

$$\eta = e_1(1-\epsilon_1)(1-\epsilon_2), \quad (27)$$

$$\bar{N} = \epsilon_1 \bar{N}_0. \quad (28)$$

We now introduce a P representation by

$$\rho = \int d^2\alpha |\alpha\rangle\langle\alpha| \rho(\alpha), \quad (29)$$

where $\rho(\alpha)$ is an operator in the space of the c_2 operators. If there is no intracavity medium (that is, the first system is an empty two-sided cavity) we can set $H_{\rm sys}$ to be $H_{\rm sys}(2)$, an operator in the second subsystem only.

The master equation (26) now becomes

$$\begin{aligned}\frac{\partial \rho(\alpha)}{\partial t} = &\frac{i}{\hbar}[\rho(\alpha), H_{\rm sys}] \\ &+\frac{\gamma_2}{2}\{2c_2\rho(\alpha)c_2^\dagger - \rho(\alpha)c_2^\dagger c_2 - c_2^\dagger c_2 \rho(\alpha)\} \\ &+\left\{\frac{\gamma_1}{2}\left(\frac{\partial}{\partial\alpha}\alpha + \frac{\partial}{\partial\alpha^*}\alpha^*\right) + \gamma_1\bar{N}\frac{\partial^2}{\partial\alpha\partial\alpha^*}\right\}\rho(\alpha) \\ &-\sqrt{\eta\gamma_1\gamma_2}\,[c_2^\dagger\alpha + c_2\alpha^*, \rho(\alpha)]. \end{aligned} \quad (30)$$

This system is equivalent to the master equation for the second system

$$\begin{aligned}\frac{\partial \rho_2}{\partial t} = &\frac{i}{\hbar}[\rho_2, H_{\rm sys}] + \frac{\gamma_2}{2}\{2c_2\rho_2 c_2^\dagger - \rho_2 c_2^\dagger c_2 - c_2^\dagger c_2 \rho_2\} \\ &-\sqrt{\eta\gamma_1\gamma_2}[c_2^\dagger\alpha(t) + c_2\alpha(t)^*, \rho_2], \end{aligned} \quad (31)$$

in which $\alpha(t)$ is a solution of the stochastic differential equation

$$d\alpha = -\frac{\gamma_1}{2}\alpha\, dt + \sqrt{\gamma_1\bar{N}}\, dv(t), \quad (32)$$

where

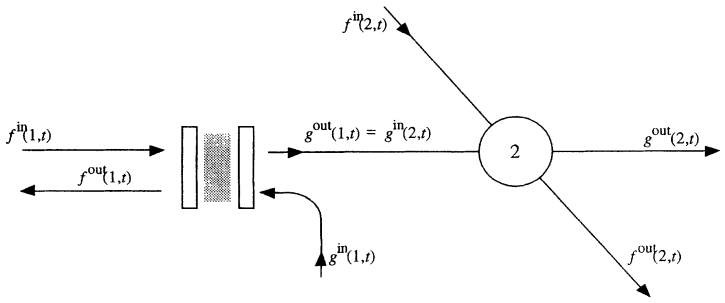

FIG. 3. Light from a two-sided harmonic oscillator coupled to a second system.

$$[dv(t)]^2 = [dv^*(t)]^2 = 0; \quad dv(t)dv^*(t) = dt. \tag{33}$$

Thus, the quantum driven systems approach is in this case equivalent to taking a system driven by a classical thermal field, $\alpha(t)$.

B. Driving by squeezed light

Here, we consider the first system to be a one-sided cavity driven by a vacuum field, as in Fig. 3. The cavity has an appropriate crystal inside which, when pumped appropriately, gives rise to a degenerate parametric amplifier [12, 11]. There is now only one input-output channel to the first system. The master equation becomes

$$\begin{aligned}\frac{\partial\rho}{\partial t} = &\frac{i}{\hbar}[\rho, H_{\rm sys}] + \frac{\gamma_1}{2}\left\{2a\rho a^\dagger - \rho a^\dagger a - a^\dagger a\rho\right\} \\ &+\frac{\gamma_2}{2}\left\{2c_2\rho c_2^\dagger - \rho c_2^\dagger c_2 - c_2^\dagger c_2\rho\right\} \\ &-\sqrt{\eta\gamma_1\gamma_2}\left\{[c_2^\dagger, a\rho] + [\rho a^\dagger, c_2]\right\},\end{aligned} \tag{34}$$

in which

$$H_{\rm sys} = \frac{i\hbar}{2}(Ea^{\dagger 2} - E^*a^2) + H_2, \tag{35}$$

where H_2 is an operator only in the second system. Similarly to the case of thermal light, we can show that the equation of motion is equivalent to (31), with the substitution $\alpha^* \to \alpha^+$, as required by a positive P representation [13, 11], which is needed to represent squeezing, and with $\alpha(t)$, $\alpha^+(t)$, satisfying the equations of motion

$$d\alpha = (-\tfrac{1}{2}\gamma_1\alpha - E\alpha^+)dt + \sqrt{E}dW_1(t), \tag{36}$$

$$d\alpha^+ = (-\tfrac{1}{2}\gamma_1\alpha^+ - E^*\alpha)dt + \sqrt{E^*}dW_2(t) \tag{37}$$

with

$$[dW_1(t)]^2 = [dW_2(t)]^2 = dt, \quad dW_1(t)\,dW_2(t) = 0.$$

This is equivalent to the equations used by Parkins and Gardiner [9] and Ritsch and Zoller [10] in considering the inhibition of atomic phase decays with finite-bandwidth squeezed light.

IV. TWO-LEVEL ATOM DRIVEN BY SQUEEZED LIGHT

The interaction of quadrature squeezed light with atoms has been a topic of considerable theoretical interest in recent years. This field of research was initiated by Gardiner [14], who showed that broad-bandwidth quadrature squeezed light can in principle inhibit the phase decay of a two-level atom, giving rise to a subnatural linewidth in the atomic fluorescence spectrum. Further analyses of other classic problems in quantum optics, such as resonance fluorescence and atomic absorption [15], yielded predictions of a variety of interesting phenomena.

However, the broad-bandwidth squeezing (or squeezed white noise) description employed in the above-mentioned work can only be regarded as an approximate model of the light produced by actual squeezed light sources, such as the degenerate parametric oscillator, which exhibit bandwidths only of the order of typical atomic transition linewidths. Recognizing this, several authors studied the influence of finite-bandwidth effects on earlier predictions using as a starting point the stochastic equations derived in Sec. III B [9, 10]. Their methods of solution were based either on stochastic simulations [9] or eigenfunction methods [10].

The coupled-systems approach described in this paper clearly offers an additional (and more direct) means of studying the response of systems to finite-bandwidth squeezed driving fields. In this section, we present some representative results to highlight the relative simplicity and potential of this approach for solving problems in which the finite-bandwidth nature of a squeezed light field has important implications.

A. Inhibition of atomic phase decays and linewidth narrowing

The master equation describing a system driven by the output light from a degenerate parametric oscillator has been given in Sec. III B. For the case in which the system under consideration is a two-level atom this equation takes the explicit form (assuming resonant excitation):

$$\begin{aligned}\frac{\partial\rho}{\partial t} = &\frac{1}{2}\left[E(a^\dagger)^2 - E^*a^2, \rho\right] + \frac{1}{2}\kappa\left(2a\rho a^\dagger - a^\dagger a\rho - \rho a^\dagger a\right) \\ &-\sqrt{\eta\kappa\gamma}\left\{[\sigma^+, a\rho] + [\rho a^\dagger, \sigma^-]\right\} \\ &+\frac{1}{2}\gamma\left(2\sigma^-\rho\sigma^+ - \sigma^+\sigma^-\rho - \rho\sigma^+\sigma^-\right).\end{aligned} \tag{38}$$

The parametric oscillator cavity is assumed to be single ended—such a configuration yields the optimum amount of squeezing in the output light. The output light is focused entirely onto the two-level atom, which may however still "see" a fraction $1 - \eta$ ($\eta \le 1$) of unsqueezed vacuum. For the squeezed light to have an appreciable influence on the atom, η should be as close to one as possible. This represents a serious practical problem, although schemes have been proposed to realize efficient coupling [16].

As is well known, fluctuations in one quadrature phase of the squeezed light are reduced below the vacuum limit, while fluctuations in the other quadrature phase are enhanced. Perfect noise reduction in the squeezed quadrature is approached in the limit $|E| \to \kappa/2$, i.e., as one approaches the threshold for parametric oscillation. In this same limit, it is important to note, however, that fluctuations in the two quadratures occur over vastly different bandwidths. In particular, the squeezed and antisqueezed quadratures are characterized by bandwidths (full width at half maximum) $\kappa + 2|E|$ and $\kappa - 2|E|$, respectively. Hence, in the limit of perfect squeezing the bandwidth of the antisqueezed quadrature approaches zero.

In the present context, this means that as the degree of squeezing is increased, one ultimately reaches a point at which the bandwidth $\kappa - 2|E|$ is smaller than the atomic linewidth γ (and hence at which white noise models are

totally inadequate). In Refs. [9, 10], it was found that this ultimately limits the extent of phase decay inhibition and line narrowing that is possible for a given cavity bandwidth κ.

In Fig. 4, we illustrate this effect by plotting the atomic fluorescence spectrum (measured through a channel upon which the squeezed light is not incident) with a series of values of the cavity bandwidth κ. In each case, the parametric oscillator is driven at 50% of threshold (corresponding to 89% squeezing at $\omega = 0$), so that $\kappa - 2|E| = 4, 2, 1$ for $\kappa = 8, 4, 2$, respectively. It is clear that once $\kappa - 2|E|$ is of the order of γ, significant line narrowing ceases to occur.

The correlation function $\langle \sigma^+(t)\sigma^-(0)\rangle_s$ (the Fourier transform of which gives the spectrum plotted in Fig. 4) was computed for each of the cases by numerically solving the master equation (39) using the methods outlined in the Appendix. In practice, we found that truncation of the cavity-mode Fock state basis to ten states was quite adequate for the description of a parametric oscillator driven at 50% of threshold—this corresponds to the mean photon number in the cavity being only $\langle a^\dagger a\rangle = 1/6$.

In terms of speed of computation the approach described here is enormously more rapid than the methods used in Refs. [9] and [10].

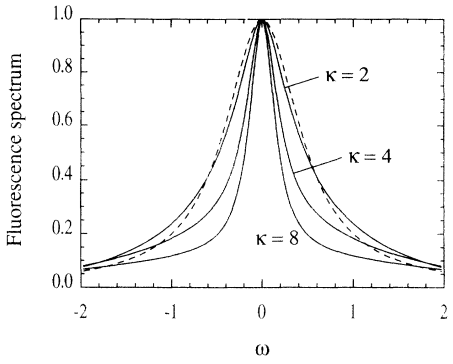

FIG. 4. Fluorescence spectrum emitted by a two-level atom driven by finite-bandwidth squeezed light from a degenerate parametric oscillator. Parameters are $\gamma = 1$, $\eta = 0.9$, and $|E|/\kappa = 0.25$. The curves have been normalized to one at $\omega = 0$ and the dashed curve is a Lorentzian of width γ. (Frequency scale in arbitrary units.)

B. Linear dependence of a two-photon transition rate using squeezed light

Squeezed light, as produced by parametric oscillators, is characterized by correlated pairs of photons. Therefore, it is quite natural to expect that the behavior of two-photon transitions in atoms should be influenced in a significant way by squeezed light. That this is indeed the case has been pointed out in studies of the effect of squeezed light on the two-photon transition rate in a three-level "ladder" system [17].

With coherent or thermal light as the driving field, two-photon excitation to the upper excited state occurs primarily, in the weak field limit, via a two-step process, with each step proportional to the driving-field intensity. Hence, the two-photon transition rate exhibits a quadratic dependence on driving-field intensity.

If, however, the driving field consists of correlated pairs of photons (coincident upon the atom within a certain correlation time), then two-photon excitation can occur essentially as a single step process proportional to the incident intensity. This leads to a linear dependence of the two-photon transition rate on intensity [17]. However, previous calculations have either been in the limit of broadband squeezed light, or have used the two-photon absorption formalism of Mollow [19], both of which are to some extent approximate, in contrast to the method presented here, which is in principle exact (at least to the extent that the Markovian assumptions used in the derivations are valid).

To highlight this fundamental difference between conventional and squeezed light excitation, we set up a model describing the following situation, which is also depicted in Fig. 5. A three-level "ladder" atom is driven by the output from a *nondegenerate* parametric oscillator (this could be either frequency or polarization nondegenerate: in the case that it is frequency nondegenerate the two cavity modes are assumed to be well separated in frequency). For simplicity we assume resonant excitation (although detunings are easily incorporated), i.e., the sum of the frequencies of the two squeezed modes is tuned to resonance with the two-photon transition $|1\rangle \to |3\rangle$, with mode a tuned to the transition $|1\rangle \to |2\rangle$ and mode b tuned to the transition $|2\rangle \to |3\rangle$.

With an appropriate unitary transformation to a rotating frame, we can write the master equation describing this configuration as

$$\begin{aligned}\frac{\partial\rho}{\partial t} &= \frac{1}{2}\left[Ea^\dagger b^\dagger - E^* ab, \rho\right] + \frac{1}{2}\kappa_a\left(2a\rho a^\dagger - a^\dagger a\rho - \rho a^\dagger a\right) + \frac{1}{2}\kappa_b\left(2b\rho b^\dagger - b^\dagger b\rho - \rho b^\dagger b\right) \\ &\quad -\sqrt{\eta\kappa_a\gamma_{21}}\left\{[\sigma_{12}^+, a\rho] + \text{H.c.}\right\} - \sqrt{\eta\kappa_b\gamma_{32}}\left\{[\sigma_{23}^+, b\rho] + \text{H.c.}\right\} \\ &\quad +\frac{1}{2}\gamma_{21}\left(2\sigma_{12}^-\rho\sigma_{12}^+ - \sigma_{12}^+\sigma_{12}^-\rho - \rho\sigma_{12}^+\sigma_{12}^-\right) + \frac{1}{2}\gamma_{32}\left(2\sigma_{23}^-\rho\sigma_{23}^+ - \sigma_{23}^+\sigma_{23}^-\rho - \rho\sigma_{23}^+\sigma_{23}^-\right). \end{aligned} \tag{39}$$

The two cavity modes are damped at the rate κ_a and κ_b, and the atomic transitions $|2\rangle \to |1\rangle$ and $|3\rangle \to |2\rangle$ have linewidths γ_{21} and γ_{32}, respectively. The fraction of input to the atom contributed by the parametric oscillator output is given by the parameter η ($\eta \le 1$).

The observable we take as a measure of two-photon absorption is the population of the upper state $|3\rangle$. This will be proportional to the two-photon absorption rate

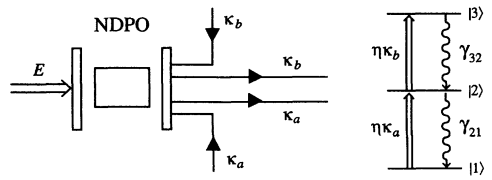

FIG. 5. Schematic diagram of the coupling between the output modes of a nondegenerate parametric oscillator (NDPO) and a three-level atom.

as calculated by Mollow [19] provided the population in this state is very small, so that no saturation effects occur. This will probably be always valid in present experiments, but if large populations occur, the assumptions in Mollow's derivation are no longer valid.

In Fig. 6, we plot the population of state $|3\rangle$ as a function of $\langle a^\dagger a\rangle_s = \langle b^\dagger b\rangle_s$ (which is directly proportional to the intensity). The linear dependence exhibited for squeezed light excitation is contrasted with the quadratic dependence obtained when the two cavity modes are uncoupled and driven independently by weak coherent fields, in such a way as to give $\langle a^\dagger a\rangle_s = \langle b^\dagger b\rangle_s$.

Our system is not entirely equivalent to that studied in previous work [17] on two-photon absorption, in that the atomic states $|3\rangle$ and $|2\rangle$ decay only to the states $|2\rangle$ and $|1\rangle$, respectively. However, as we see, the same kind of intensity dependent behavior is found to occur.

Again, it should be emphasized that the coupled systems description given by the master equation above requires no assumptions regarding the relative magnitudes of the atomic state linewidths and the squeezing bandwidth. This flexibility with respect to the choice of parameters has enabled us to consider a number of different regimes and it is clear that a comprehensive study of this system would be needed to fully characterize its behavior. However, for this initial study we confine ourselves to a particular choice of parameters that we have found

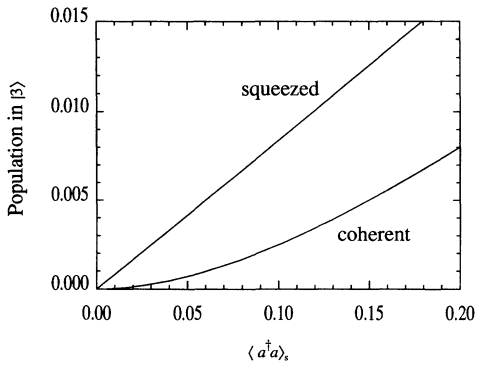

FIG. 6. Population of the upper atomic state $|3\rangle$ as a function of the cavity mode photon number $\langle a^\dagger a\rangle_s$, which is a direct measure of the incident intensity. Parameters for this figure are $\kappa_a = \kappa_b = 2$, $\eta = 0.5$, $\gamma_{21} = 5$, $\gamma_{32} = 10$. The case of excitation with correlated squeezed light is contrasted with the case of independent coherent excitation of the two transitions.

to produce results of the nature described earlier, i.e., a linear intensity dependence of the upper state population.

V. TWO-LEVEL ATOM DRIVEN BY ANTIBUNCHED LIGHT FROM ANOTHER ATOM

We consider now the numerical analysis of further problems for which the coupled-systems formulation of the previous sections is particularly suited and, in fact, quite essential. Indeed, the first scenario we shall consider—an atom driven by antibunched light—constitutes a problem for which solutions were unknown until the coupled systems approach was applied to it by Gardiner [4], although Knight and Pegg [18] gave a perturbative treatment of a three-level atom driven by antibunched light, aimed at using the three-level atom as a two-photon spectral analyzer.

As in that work, we begin by taking our source of antibunched light to be a single two-level atom. Historically, this was the first system studied in the context of antibunching and it can be regarded as the prototypical antibunched-light source. There are still significant experimental problems to be solved before the coupling of two atoms in a manner corresponding to the present formulation can, of course, be achieved in practice. We note, though, that alternative sources of antibunched light, such as cavity QED configurations which produce nonclassical light in directed and controllable beams [20], would be more amenable to effective coupling with atomic samples. But it must be emphasized that this paper will demonstrate that an accurate modeling of the details of the system producing the nonclassical light must be carried out before we can say with confidence that we know what the effect of such a source would be on a two-level atom.

Given that our source of antibunched light is a two-level atom, a pumping mechanism must be provided to excite this atom and induce fluorescence from which the source field is derived. The two distinct possibilities that we shall consider are (i) coherent pumping provided by incident light from a laser, and (ii) incoherent pumping provided by finite-bandwidth thermal light.

A. Coherent excitation of the source atom

1. Master equation

The configuration that we shall consider is shown schematically in Fig. 7, where we illustrate the various input, output, and coupling channels for the case of coherent excitation of the source atom. The master equation describing this situation takes the form

$$\begin{aligned}\frac{\partial\rho}{\partial t} &= \frac{1}{2}\gamma_1\left(2\sigma_1^-\rho\sigma_1^+ - \sigma_1^+\sigma_1^-\rho - \rho\sigma_1^+\sigma_1^-\right)\\ &\quad -\sqrt{\epsilon_1\gamma_1}[E\sigma_1^+ - E^*\sigma_1^-,\rho]\\ &\quad -\sqrt{(1-\epsilon_1)(1-\epsilon_2)\gamma_1\gamma_2}\left([\sigma_2^+,\sigma_1^-\rho] + [\rho\sigma_1^+,\sigma_2^-]\right)\\ &\quad +\frac{1}{2}\gamma_2\left(2\sigma_2^-\rho\sigma_2^+ - \sigma_2^+\sigma_2^-\rho - \rho\sigma_2^+\sigma_2^-\right). \qquad (40)\end{aligned}$$

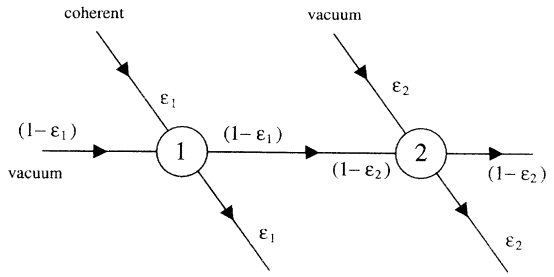

FIG. 7. Schematic diagram of the coupling between a coherently-driven atom (1) and a second atom (2). The various input, output, and coupling channels are discussed in the text.

The (classical) coherent electric field E is incident upon atom 1 through the channel labeled ϵ_1. This coherent field is not incident upon atom 2. Antibunched light emitted from atom 1 into channel $(1-\epsilon_1)$ provides the light source for atom 2 with which it is coupled through channel $(1-\epsilon_2)$. The (vacuum input) channel ϵ_2 provides an observation channel for the light emitted from atom 2.

To solve the master equation we use direct numerical integration on a computer. Application of the quantum regression theorem yields all of the correlation functions and spectra of interest. More details of our computational technique are given in the Appendix.

2. *General features*

The property of antibunching in the light emitted from a two-level atom is a consequence of the finite time required for the atom to be reexcited from its ground state following the emission of a photon. This is manifested in the stationary normally-ordered intensity correlation function of the emitted light. This function is directly related to photon-counting measurements, representing the conditional probability of counting a second photon at a time t after the initial detection of a photon. For a two-level atom this function is identically zero for $t = 0$.

A generalization of this correlation function which we shall compute for the two-atom system at hand is given by

$$\langle : I_i(t) I_j(0) : \rangle_s = \beta_i \beta_j \mathrm{Tr}\left[\sigma_i^+ \sigma_i^- V(t)\left\{\sigma_j^- \rho_s \sigma_j^+\right\}\right], \quad (41)$$

where $i, j = 1, 2$ (first or second atom), $V(t)$ is the (two-sided) evolution operator, such that $V(t)\rho(t') = \rho(t+t')$, and ρ_s is the stationary solution of the master equation. These functions can be interpreted as the conditional probability of counting a photon from atom i a time t after counting a photon from atom j. Their measurement would correspond to photon-counting measurements on the output fields in the channels $(1-\epsilon_1)$ and ϵ_2 [i.e., $\beta_1 = (1-\epsilon_1)\gamma_1$ and $\beta_2 = \epsilon_2\gamma_2$]; these fields are not contaminated with nonvacuum input fields, which simplifies the analysis, though the analysis of other fields could also be of interest.

The most significant qualitative features of the intensity correlation functions are similar for coherent and incoherent excitation of the source atom, so we shall simply consider the case of coherent excitation and summarize the significant features noted previously by Gardiner [4]. An example is illustrated in Fig. 8, where we plot the normalized intensity correlation functions,

$$g_{ij}^{(2)}(t) = \frac{\langle : I_i(t) I_j(0) : \rangle_s}{\langle I_i \rangle_s \langle I_j \rangle_s}, \quad (42)$$

for two different values of the coherent field strength. These plots present a typical set of results and exhibit the following features.

(i) A "retardation" of the evolution of $g_{22}^{(2)}(t)$ in comparison to that of $g_{11}^{(2)}(t)$. This is not a consequence of the time delay τ between the two atoms; rather it simply reflects the different rates of reexcitation experienced by the two atoms.

(ii) A pronounced anticorrelation in $g_{21}^{(2)}(0)$ [i.e., $g_{21}^{(2)}(0) < 1$]. This arises because of the antibunching. If a photon is detected from atom 1, then it is not available to excite atom 2. The anticorrelation is not perfect, since emission depends on the excitation of each atom—however, because of the antibunching, if a photon was counted from atom 1, then there was a reduced probability of there having been one in the immediate past to excite atom 2. This probability is dependent upon

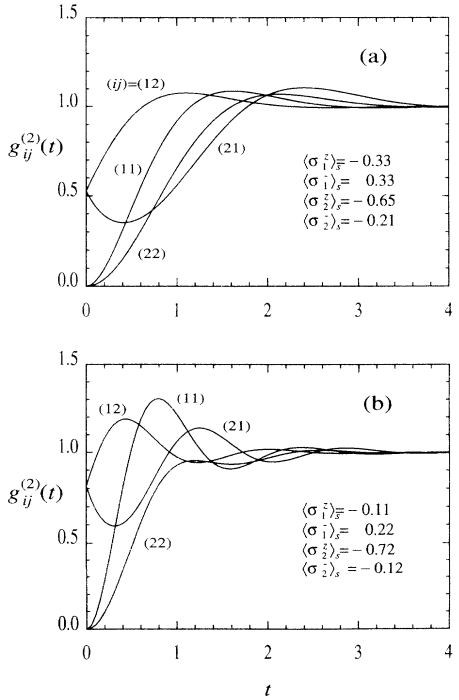

FIG. 8. Intensity correlation function $g_{ij}^{(2)}(t)$ for a two-level atom driven by light from a coherently driven two-level atom, with (a) $\sqrt{\epsilon_1\gamma_1}E = 1$, and (b) $\sqrt{\epsilon_1\gamma_1}E = 2$, where $\epsilon_1 = 0.5$ and $\gamma_1 = 2$. The other parameters from master equation (41) are $\epsilon_2 = 0.5$, $\gamma_2 = 2$. (Time scale in arbitrary units.)

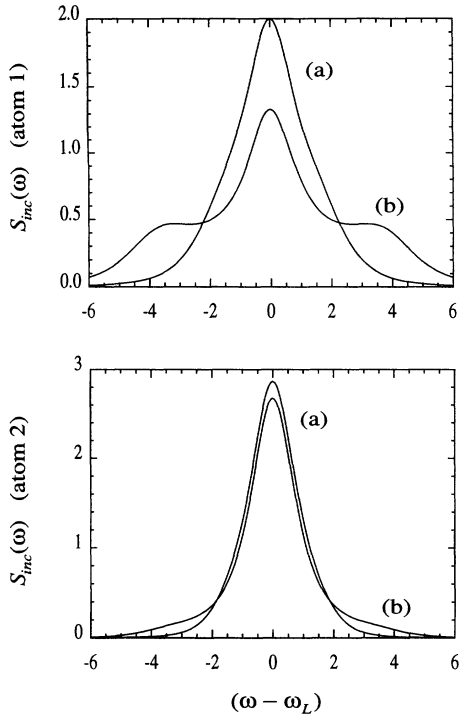

FIG. 9. Incoherent fluorescence spectra emitted from atoms 1 and 2 for the parameters of the previous figure. Curves (a) and (b) correspond to $\sqrt{\epsilon_1\gamma_1}E = 1$ and $\sqrt{\epsilon_1\gamma_1}E = 2$, respectively. The spectra are normalized by the total incoherent intensity. (Frequency scale in arbitrary units.)

the rate of excitation of atom 1, as evidenced by the decrease in the anticorrelation at $t = 0$ that occurs with an increase in the coherent driving field strength [Fig. 8(b)].

(iii) This anticorrelation initially becomes more pronounced as t increases. This is because there will be no further photons to excite atom 2 in the time immediately following the emission, i.e., atom 1 is unable to provide a driving field for atom 2 until it has recovered some excitation. Eventually, of course, photons do appear, and $g_{21}^{(2)}(t)$ approaches a value representing zero correlation.

(iv) In contrast, the correlation function $g_{12}^{(2)}(t)$ tends to mirror the behavior of $g_{11}^{(2)}(t)$, simply reflecting the fact that excitation of atom 1 is provided by a coherent (Poissonian) light field.

Steady-state values of the atomic inversion and polarization are also given in Fig. 8, and it is interesting to note that the degree of excitation of atom 2 decreases with an increase in the strength of the coherent field driving atom 1. This reflects the changing spectral distribution of the light emitted from atom 1, as shown in Fig. 9, where we plot the incoherent fluorescence spectra for the two cases (the spectra are normalized by the respective total incoherent intensities). The Rabi sidebands that appear for $E = 2$ [Fig. 9(a)] are out of resonance with the transition frequency of atom 2, and hence the power contained in these sidebands has a limited influence on the excitation of atom 2.

B. Incoherent excitation of the source atom

1. Master equation

We would like to test to what extent the antibunched nature of the light emitted from the first atom characterizes the nature of the photon counting from the second atom. To do this we shall show that we can produce a light beam from the first atom which has the same intensity and $g^{(2)}(t)$ as that emitted when the light incident is coherent, but is otherwise quite different.

Let us consider excitation of atom 1 by a thermal light field with finite bandwidth. The configuration we shall model is illustrated in Fig. 10 and the corresponding master equation is given by

$$\frac{\partial\rho}{\partial t} = \kappa(\bar{N}+1)\left(2a\rho a^\dagger - a^\dagger a\rho - \rho a^\dagger a\right) + \kappa\bar{N}\left(2a^\dagger\rho a - aa^\dagger\rho - \rho aa^\dagger\right)$$
$$-\sqrt{2\kappa\eta_1\gamma_1}\left([\sigma_1^+, a\rho] + [\rho a^\dagger, \sigma_1^-]\right) + \frac{1}{2}\gamma_1\left(2\sigma_1^-\rho\sigma_1^+ - \sigma_1^+\sigma_1^-\rho - \rho\sigma_1^+\sigma_1^-\right)$$
$$-\sqrt{\eta_2\gamma_1\gamma_2}\left([\sigma_2^+, \sigma_1^-\rho] + [\rho\sigma_1^+, \sigma_2^-]\right) + \frac{1}{2}\gamma_2\left(2\sigma_2^-\rho\sigma_2^+ - \sigma_2^+\sigma_2^-\rho - \rho\sigma_2^+\sigma_2^-\right). \quad (43)$$

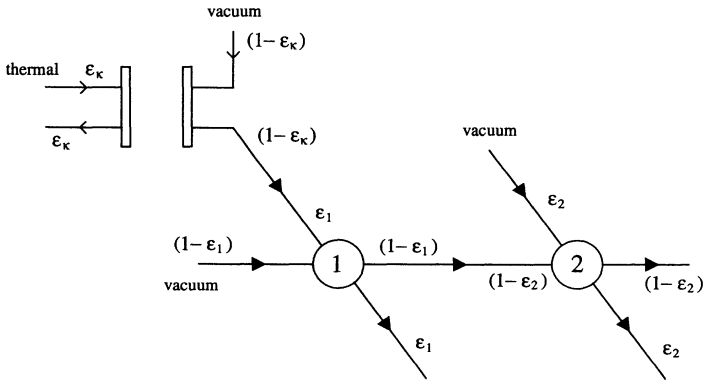

FIG. 10. Schematic diagram of the coupling between a thermally driven cavity and two atoms (1,2). The various input, output, and coupling channels are discussed in the text.

The finite-bandwidth thermal field is provided by the output from a cavity driven (through the input channel denoted by ϵ_κ) by a broadband, or "white noise," thermal field. The cavity output through channel $(1-\epsilon_\kappa)$ is coupled to atom 1 through channel ϵ_1. Again, this driving field is not incident upon atom 2. The coupling parameters are given by $\eta_1 = (1-\epsilon_\kappa)\epsilon_1$ and $\eta_2 = (1-\epsilon_1)(1-\epsilon_2)$.

Our choice of a finite-bandwidth thermal field is motivated by the need to produce a $g^{(2)}(t)$ in which the initial time dependence is quadratic, as in the case of light from a coherently driven atom. A broadband thermal field would inevitably produce an initial linear t dependence. We shall see that by suitably adjusting the bandwidth of the driving field, we can closely match correlation functions for the two different cases of coherent and incoherent excitation of the source atom, so that we may carry out the following comparison between the effects of different kinds of antibunched light.

2. *Comparison with coherent excitation: different kinds of antibunched light*

The intensity of a light beam and fluctuations in the intensity are properties that one might typically measure, using photon counting, in order to achieve some degree of characterization of the light beam. In the case of antibunched light, both as a driving field (from atom 1) and as the emission induced (on atom 2) by this driving field, it is interesting to consider to what extent the photon counting properties of the induced emission are determined by those of the driving field. It is primarily for this reason that we want to consider finite-bandwidth thermal excitation of the source atom, since this allows us to make a controlled comparison of the effects of two different sources of antibunched light. In particular, we can compare the cases of purely coherent [Eq.(41)] and purely incoherent [Eq.(44)] thermal excitation of atom 1 when the intensity of the light driving atom 2,

$$\eta_2\gamma_1\langle\sigma_1^+\sigma_1^-\rangle_s\ , \tag{44}$$

$[\eta_2 = (1-\epsilon_1)(1-\epsilon_2)]$ and the intensity correlation function,

$$g_{11}^{(2)}(t) = \frac{\langle\sigma_1^+\sigma_1^+(t)\sigma_1^-(t)\sigma_1^-\rangle_s}{\langle\sigma_1^+\sigma_1^-\rangle_s^2}\ , \tag{45}$$

are as close as possible the same for both situations. The two different driving fields for atom 2 can then be regarded as having identical antibunching properties.

Such a comparison is presented in Figs. 11(a) and 11(b), where we plot the functions $g_{ij}^{(2)}(t)$ for two different values of the intensity $\eta_2\gamma_1\langle\sigma_1^+\sigma_1^-\rangle_s$ emitted by atom 1 into the coupling channel $\eta_2\gamma_1$. By a suitable choice of parameters, we are able to closely match $g_{11}^{(2)}(t)$ and $\eta_2\gamma_1\langle\sigma_1^+\sigma_1^-\rangle_s$ for the two cases (such that they would quite certainly be indistinguishable in an experiment).

The curves describing $g_{ij}^{(2)}(t)$ for $(ij) = (12), (21), (22)$ are clearly different for the two cases, as are the respective intensities of light emitted from atom 2—values of the excited state population for atom 2 are $\langle\sigma_2^+\sigma_2^-\rangle_s =$ 0.0651 (thermal), 0.0929 (coherent) for Fig. 11(a), and $\langle\sigma_2^+\sigma_2^-\rangle_s = 0.108$ (thermal), 0.341 (coherent) for Fig. 11(b).

These results demonstrate that the photon-counting properties of the light emitted by an atom driven with antibunched light depend on properties of the antibunched light other than those specified by $g_{11}^{(2)}(t)$ and $\eta_2\gamma_1\langle\sigma_1^+\sigma_1^-\rangle_s$. Indeed, the spectral properties of the antibunched driving field are quite different for the two cases, as illustrated by Fig. 12 in which we plot the incoherent fluorescence spectrum emitted by atom 1. Properties displayed in such spectra must evidently be taken into consideration when characterizing an antibunched light field with respect to its influence on the purely photon-counting properties of light emitted by the atoms upon which it is incident. Indeed the question does arise as to how one should characterize an arbitrary light beam in terms of a few parameters.

VI. TWO-LEVEL ATOM DRIVEN BY A COUPLED ATOM-CAVITY SYSTEM

In this section, we consider a source of light derived from a system that is presently at the forefront of theoretical and experimental quantum optics research. That

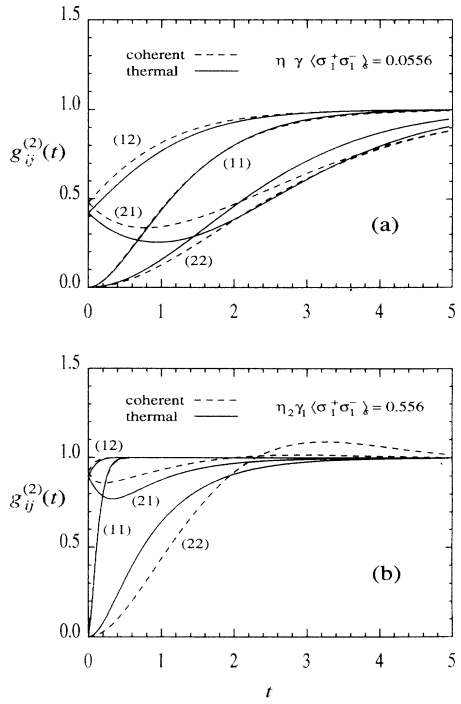

FIG. 11. Comparison of intensity correlation functions for coherent and thermal excitation of atom 1. The function $g_{11}^{(2)}(t)$ and the intensity $\eta_2\gamma_1\langle\sigma_1^+\sigma_1^-\rangle$ $[\eta_2 = (1-\epsilon_1)(1-\epsilon_2)]$ have been matched for the two cases. Parameters for the two figures, referring to the master equations (43) and (40), are (a) thermal: $\kappa = 1.15$, $\bar{N} = 0.207$, $\eta_1 = 0.25$, $\gamma_1 = 0.8$, $\eta_2 = 0.3125$, $\gamma_2 = 1$; coherent: $\gamma_1 = 2$, $\sqrt{\epsilon_1\gamma_1}E = 0.25$, $\epsilon_2 = 0.5$, $\gamma_2 = 1$; (b) thermal: $\kappa = 11.5$, $\bar{N} = 0.207$, $\eta_1 = 0.25$, $\gamma_1 = 8$, $\eta_2 = 0.3125$, $\gamma_2 = 1$; coherent: $\gamma_1 = 20$, $\sqrt{\epsilon_1\gamma_1}E = 2.5$, $\epsilon_2 = 0.5$, $\gamma_2 = 1$. (Time scale in arbitrary units.)

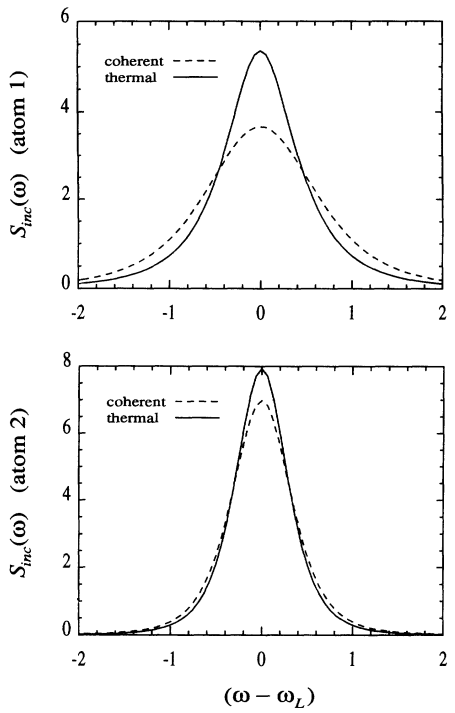

FIG. 12. Incoherent fluorescence spectra emitted from atom 1 and atom 2, for the parameters of Fig. 11(a). The spectra are normalized by the total incoherent intensity. (Frequency scale in arbitrary units.)

system is a single two-level atom strongly coupled to a single mode of the electromagnetic field inside a cavity. In spite of its apparent simplicity, this system has been shown theoretically to possess a rich variety of properties including squeezing, antibunching, and optical bistability [21, 22]. Interesting schemes have been proposed for the generation of Fock states and coherent superposition (or "Schrödinger cat") states of the field [23].

Recent experiments realizing such an idealized atom-cavity system [24] bring into consideration the question of how the light generated by this system might interact with other quantum optical systems. The coupled-systems approach offers a means of addressing this question, taking into account the full dynamics of the atom-cavity driving system and allowing for the great variety of statistical properties exhibited by the light in different operating regimes.

We again consider the influence of the source light on a single two-level atom, as depicted in Fig. 13. The master

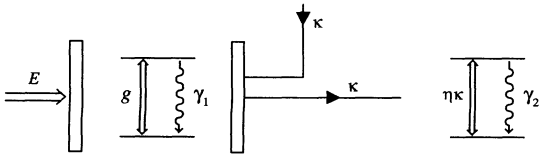

FIG. 13. Configuration for a two-level atom driven by light from a coherently driven atom-cavity system. The transmissivity of the output mirror is much larger than that of the other mirror, and so the cavity is considered to be single ended.

equation describing the complete system can be divided into three contributions:

$$\frac{\partial\rho}{\partial t} = \left(\frac{\partial\rho}{\partial t}\right)_{\text{source}} + \left(\frac{\partial\rho}{\partial t}\right)_{\text{atom}} + \left(\frac{\partial\rho}{\partial t}\right)_{\text{coupling}} . \quad (46)$$

The atom-cavity system is driven by a coherent field entering through one of the mirrors. Losses through this mirror are assumed to be negligible compared to losses through the other mirror which serves as the output channel for the source light. Thus, we write the master equation for the driven atom-cavity source as

$$\begin{aligned}\left(\frac{\partial\rho}{\partial t}\right)_{\text{source}} &= [Ea^\dagger - E^* a, \rho] + g[a^\dagger\sigma_1^- - \sigma_1^+ a, \rho] \\ &\quad + \frac{1}{2}\gamma_1\left(2\sigma_1^-\rho\sigma_1^+ - \sigma_1^+\sigma_1^-\rho - \rho\sigma_1^+\sigma_1^-\right) \\ &\quad + \kappa\left(2a\rho a^\dagger - a^\dagger a\rho - \rho a^\dagger a\right), \end{aligned} \quad (47)$$

where E is the effective coherent field amplitude, g is the atom-cavity coupling strength, γ_1 is the atomic spontaneous emission linewidth, and κ is the loss rate through the output mirror.

The second two-level atom outside the cavity may possibly be different from the cavity-confined atom, and so the master equation describing this atom is written as

$$\begin{aligned}\left(\frac{\partial\rho}{\partial t}\right)_{\text{atom}} &= -\frac{1}{2}i[\Delta\sigma_2^z, \rho] \\ &\quad + \frac{1}{2}\gamma_2\left(2\sigma_2^-\rho\sigma_2^+ - \sigma_2^+\sigma_2^-\rho - \rho\sigma_2^+\sigma_2^-\right), \end{aligned} \quad (48)$$

with $\Delta = \omega_2 - \omega_1$, where ω_1 and ω_2 are the transition frequencies for the cavity-confined atom and the external atom, respectively.

Finally, the coupling between the output light from the cavity and the external atom is described by the term

$$\begin{aligned}&\left(\frac{\partial\rho}{\partial t}\right)_{\text{coupling}} \\ &\quad = -\sqrt{(2\kappa)(\eta\gamma_2)}\left([\sigma_2^+, a\rho] + [\rho a^\dagger, \sigma_2^-]\right), \end{aligned} \quad (49)$$

where η gives the fraction of input to atom 2 contributed by the cavity output, i.e., it allows for the possibility that atom 2 may not (and usually will not) be exclusively coupled to the field emitted from the cavity.

Again, the master equation can be solved quickly and efficiently by numerical integration on a computer. A comprehensive characterization of the light emitted from the cavity and incident on the external atom is possible through straightforward computations (via the quantum regression theorem) of the intensity correlation function (from which we may also compute the intensity fluctuation spectrum), quadrature squeezing spectra, and the fluorescence spectrum.

Photon statistics

As mentioned above, the light generated by an atom-cavity system can exhibit a great variety of statistical properties depending on the particular operating regime. In keeping with previous sections, we shall concentrate

on the influence of this light on an atom with regards to its photon-counting properties. Again, it is in this area, where higher-order moments of system operators are crucial, that the coupled-systems approach offers a new insight.

A particularly interesting range of photon statistics in the output from an atom-cavity system is found in the limit of weak driving fields [22, 25], such that $\langle a^\dagger a\rangle_s \ll 1$. This is illustrated in Fig. 14(a), where we plot the intensity correlation function for the light emitted from the cavity,

$$g^{(2)}(t) = \frac{\langle a^\dagger a^\dagger(t)a(t)a\rangle_s}{\langle a^\dagger a\rangle_s^2}, \tag{50}$$

for a range of parameters (such that $\langle a^\dagger a\rangle \ll 1$). As the coupling strength g is increased, we observe a transition from antibunched to bunched light, with a "dip" appearing in $g^{(2)}(t)$ at nonzero times. This dip has been studied previously [22, 25] and arises from the electric field passing through zero after a photon emission. This is the result of a subtle interference effect between the driving coherent field and the atomic dipole (or reaction) field.

We note that the cavity output fields corresponding to curves (a)–(d) are all nonclassical fields by virtue of the fact that $g^{(2)}(0) < 1$. In the case of curve (e) this is not so apparent, as classical fields can be devised with a similar behavior. However, it can be shown that classical fields must satisfy the inequality

$$\frac{\langle a^\dagger a^\dagger(t)a(t)a\rangle_s}{|\langle a^\dagger(t)a\rangle_s|^2} \geq 1 \tag{51}$$

for all t [26]. This inequality is violated at certain times by the field corresponding to curve (e) and thus it must also be regarded as nonclassical.

In fact, we find that the violation is very large, since direct computation shows that to better than 1%

$$|\langle a^\dagger(t)a(0)\rangle|^2 \approx |\langle a^\dagger(0)a(0)\rangle|^2 \tag{52}$$

so that in this case, the left-hand side of the inequality (51) is essentially the same as $g^{(2)}(t)$. As can be seen from Fig. 14(a) in all cases, and in curve (e) in particular, $g^{(2)}(t)$ can be very much less than 1, thus violating the inequality (51). It can be seen that the light appears to be, from the point of view of second-order statistics, almost coherent—the approximate equality (52) shows this. Nevertheless, the fourth-order correlation function, $g^{(2)}(t)$, which reflects a genuine quantum property, is very far from that of a coherent field, and in a quantum sense, this field is *very* different from a coherent field.

The influence of such light on a two-level atom, or, more particularly, on the photon statistics of the light emitted from the atom, is shown in Fig. 14(b), where we plot

$$g^{(2)}(t) = \frac{\langle \sigma_2^+\sigma_2^+(t)\sigma_2^-(t)\sigma_2^-\rangle_s}{\langle \sigma_2^+\sigma_2^-\rangle_s^2}. \tag{53}$$

The most significant feature illustrated by this figure is a dramatic enhancement of the antibunching near $t = 0$.

Given that a photon has been counted from atom 2, one knows that a photon must have been emitted from the cavity a time $\sim \gamma_2^{-1}$ earlier. If the probability for the emission of a second photon from the cavity is small after this time delay [e.g., if $g^{(2)}(t)$ dips close to zero for t of the order of γ_2^{-1}], then there is little chance of atom 2 being excited again immediately following its first emission. Hence, the intensity correlation function for atom 2 remains close to zero for an extended length of time. This means that antibunching in the light emitted from atom 2 can be enhanced even when the input field

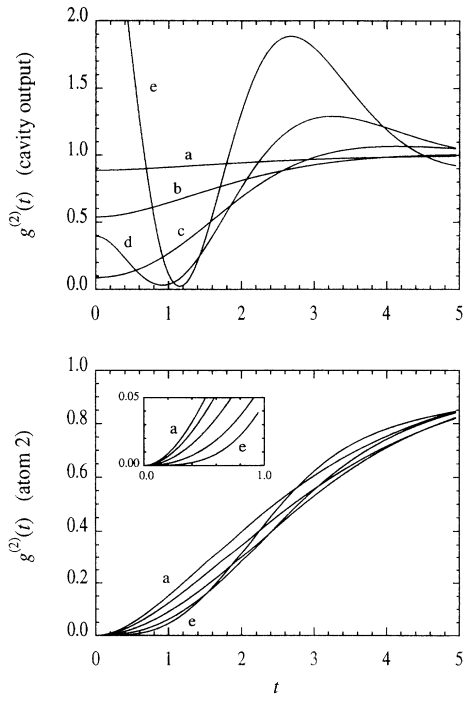

FIG. 14. Intensity correlation function for the light emitted from the cavity and atom 2. The parameters are $\kappa = 1$, $\gamma_1 = \gamma_2 = 1$, $gE = 0.04$, $\eta = 0.5$, and (a) $g = 0.4$, (b) $g = 0.6$, (c) $g = 0.8$, (d) $g = 1.0$, (e) $g = 1.2$. The inset in (b) shows a magnified view of the region from $t = 0$ to $t = 1$. (Time scale in arbitrary units.)

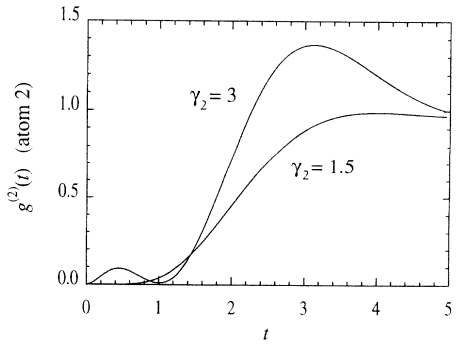

FIG. 15. Intensity correlation function for the light emitted from atom 2. The parameters are $\kappa = 1$, $\gamma_1 = 1$, $g = 1.2$, $E = 0.033$, $\eta = 0.5$, and $\gamma_2 = 1.5, 3$. (Time scale in arbitrary units.)

is very strongly bunched [Fig. 14, curve (e)].

Even more dramatic effects can be found by varying the value of γ_2, as shown in Fig. 15. For $\gamma_2 = 1.5$, $g^{(2)}(t)$ is essentially zero until $t \simeq 0.7$, while for $\gamma_2 = 3$ the statistics of the light emitted from atom 2 begin to "follow" those of the incident field, with a pronounced dip appearing near $t \simeq 1$. For large γ_2, the behavior of atom 2 can evidently be likened to that of an idealized photodetector.

VII. CONCLUSIONS

We have developed the coupled-systems approach in this paper to such an extent that its full practical utility can be seen. The next step must be calculations directly related to practical experiments. We can say with confidence that provided the mechanism for producing a given nonclassical light beam is known, its effect on any system can be predicted. However the range of possibilities of nonclassical sources, systems to illuminate, and effects to observe is enormous, and we may well find surprises as we investigate more deeply. We have investigated squeezed light (both single mode and two mode), antibunched light of two different kinds, and the highly nonclassical light from atom-cavity systems. The only major problem one would expect from realistic systems is the size of the matrices which could possibly arise, since in all our examples the number of atomic levels has been small, as have the number of oscillator states required to model the optical cavities. It will be necessary to devise better technical methods where these conditions are not met.

ACKNOWLEDGMENTS

We wish to thank Peter Zoller and Howard Carmichael for illuminating discussions, and the New Zealand Foundation for Research, Science and Technology for financial support under Contract No. UOW306.

APPENDIX: NUMERICAL INTEGRATION OF THE MASTER EQUATION

In coupling together a number of quantum optical systems and formulating a master equation description, we are invariably faced with a model involving a large number of basis states. If we do not wish to make any further approximations beyond the master equation, then we must resort to numerical solutions.

In this Appendix, we briefly outline the approach that we have taken to solving the master equation numerically. We have found our approach to be a reasonably practical and efficient means of obtaining solutions on modern workstations for problems involving up to 200 basis states. We also believe that its relative simplicity and generality are worthy of note.

The master equation can always be written in the general form

$$\frac{\partial \rho}{\partial t} = (H\rho + \rho H^\dagger) + \sum_{k=1}^{m} O_k \rho O_k^\dagger \equiv L\rho, \tag{A1}$$

where H and $\{O_k, k = 1, m\}$ are certain (problem specific) operators. For a system spanned by N basis states, these operators can be written as $N \times N$ matrices. Repeated evaluation of $L\rho$ as a function of time constitutes the major computational effort required in numerically solving the master equation.

Our approach to the computation of $L\rho$ is very direct, in that it is based simply on the evaluation of the matrix products appearing in $L\rho$. Multiplication of large matrices is often very time consuming, but here we are able to make use of the fact that the matrices H and $\{O_k, k = 1, m\}$ are typically very sparse; in fact, for all of the cases that we have considered, each matrix O_k contains at most one nonzero element per row, while H possesses at most 3 or 4 nonzero elements per row.

More specifically, our approach can be divided into the following series of steps.

(i) Within a program, functions of two integers (indices) are set up to specify the elements of each of the various matrix operators H and $\{O_k, k = 1, m\}$ appearing in $L\rho$; the number of functions (operators) and their precise nature depends on the particular problem we are considering. Hence, the master equation is essentially specified entirely in terms of the matrix operators appearing in $L\rho$. This approach avoids the need to derive and then program equations of motion governing the evolution of individual density matrix elements. Such a matrix operator-based approach is very straightforward to follow and to generalize.

(ii) Given these functions, at the beginning of the program we store the positions and values of the nonzero elements of H and $\{O_k, k = 1, m\}$. For a particular O_k this requires only two (one dimensional) arrays of length N.

(iii) Noting that $\rho H^\dagger \equiv (H\rho)^\dagger$ and $O_k \rho O_k^\dagger \equiv O_k(O_k\rho)^\dagger$, we reduce all of the matrix operations required in the evaluation of $L\rho$ to matrix products of the form $H\rho$ or $O_k\rho$. Using the information gained in step (ii) (regarding the positions of the nonzero elements of the matrices H and O_k), the various matrix multiplications are performed in such a way that only multiplications involving the nonzero elements of H and O_k are carried out. A caveat to our approach to computing these matrix products is that we assume nothing about the elements of ρ. We have not yet attempted to optimize our approach in this respect, but it would seem that further improvement should be possible.

(iv) Finally, given our algorithm for evaluating $L\rho$, we employ a fourth-order Runge-Kutta integration scheme (with variable step size) to compute the time evolution of the density matrix. Typically, we make use of the NAG (Numerical Algorithms Group) computer routine D02BBF or the Numerical Recipes routine ODEINT [27].

Our programs are run typically on a DECstation 5000 or IBM RISC 6000 computer. Run times obviously vary depending on the dimension of a problem and the magnitude of the parameters involved. However, for problems involving approximately 100 basis states, stationary density matrices are typically obtained in times of the order of minutes (two time correlation functions require essentially the same amount of time to evaluate).

[1] C.W. Gardiner and M.J. Collett, Phys. Rev. A **31**, 3761 (1985).
[2] B. Yurke and J.S. Denker, Phys. Rev. A **29**, 1419 (1984).
[3] M.I. Kolobov and I.V. Sokolov, Opt. Spektrosk. **62**, 112 (1987) [Opt. Spectrosc. (USSR) **62**, 69 (1987)].
[4] C.W. Gardiner, Phys. Rev. Lett. **70**, 2269 (1993).
[5] H.J. Carmichael, Phys. Rev. Lett. **70**, 2273 (1993).
[6] *Squeezed States of the Electromagnetic Field*, edited by H.J. Kimble and D.F. Walls [J. Opt. Soc. Am. B **4**, 1450 (1987)].
[7] *Squeezed Light*, edited by P.L. Knight and R. Loudon [J. Mod. Opt. **34**, 709 (1987)].
[8] *Quantum Noise Reduction in Optical Systems*, edited by C. Fabre and E. Giacobino [Appl. Phys. B **55**, 189 (1992)].
[9] A.S. Parkins and C.W. Gardiner, Phys. Rev. A **37**, 3867 (1988).
[10] H. Ritsch and P. Zoller, Phys. Rev. Lett. **61**, 1097 (1988); Phys. Rev. A **38**, 4657 (1988).
[11] C.W. Gardiner, *Quantum Noise* (Springer, Heidelberg, 1991).
[12] M.J. Collett and C.W. Gardiner, Phys. Rev. A **30**, 1386 (1984).
[13] P.D. Drummond and C.W. Gardiner, J. Phys. A **13**, 2353 (1980).
[14] C.W. Gardiner, Phys. Rev. Lett. **56**, 1917 (1986).
[15] H.J. Carmichael, A.S. Lane, and D.F. Walls, Phys. Rev. Lett. **58**, 2539 (1987); H. Ritsch and P. Zoller, Opt. Commun. **64**, 523 (1987); **66**, 333(E) (1988); S. An, M. Sargent, and D.F. Walls, *ibid.* **67**, 373 (1988); J.-M. Courty and S. Reynaud, Europhys. Lett. **10**, 237 (1989).
[16] A.S. Parkins and C.W. Gardiner, Phys. Rev. A **40**, 3796 (1989); **42**, 5765(E) (1990).
[17] J. Gea-Banacloche, Phys. Rev. Lett. **62**, 1603 (1989); J. Javanainen and P. L. Gould, Phys. Rev. A **41**, 5088 (1990); Z. Ficek and P.D. Drummond, *ibid.* **43**, 6247 (1991); **43**, 6258 (1991).
[18] P.L. Knight and D.T. Pegg, J. Phys. B **15**, 3211 (1982).
[19] B.R. Mollow, Phys. Rev. **175**, 1555 (1968).
[20] G. Rempe, R.J. Thompson, R.J. Brecha, W.D. Lee, and H.J. Kimble, Phys. Rev. Lett. **67**, 1727 (1991).
[21] H.J. Carmichael, Phys. Rev. Lett. **55**, 2790 (1985); C.M. Savage and H.J. Carmichael, IEEE J. Quantum Electron. **24**, 1495 (1988).
[22] P.R. Rice and H.J. Carmichael, IEEE J. Quantum Electron. **24**, 1351 (1988).
[23] M. Brune, S. Haroche, V. Lefevre, J.M. Raimond, and N. Zagury, Phys. Rev. Lett. **65**, 976 (1990); M.J. Holland, D.F. Walls, and P. Zoller, *ibid.* **67**, 1716 (1991); M. Brune, S. Haroche, J.M. Raimond, L. Davidovich, and N. Zagury, Phys. Rev. A **45**, 5193 (1992); A.S. Parkins, P. Marte, P. Zoller, and H.J. Kimble (unpublished).
[24] R.J. Thompson, G. Rempe, and H.J. Kimble, Phys. Rev. Lett. **68**, 1132 (1992).
[25] H.J. Carmichael, R.J. Brecha, and P.R. Rice, Opt. Commun. **82**, 73 (1991).
[26] C.W. Gardiner, *Quantum Noise* (Springer, Heidelberg, 1991), Sec. 8.3.4(d).
[27] W.H. Press, B.P. Flannery, S.A. Teukolsky, and W.T. Vetterling, *Numerical Recipes: The Art of Scientific Computing* (Cambridge University Press, Cambridge, England, 1988).

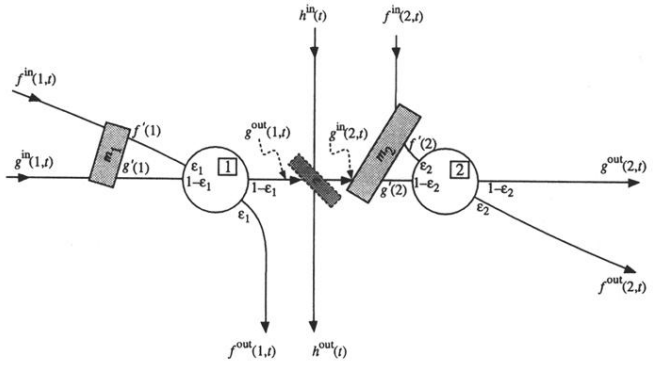

FIG. 2. Arrangements required to account for imperfect coupling. The systems are considered to have two input-output channels. The corresponding fields are coupled with strengths $\sqrt{\epsilon_i}$, $\sqrt{1-\epsilon_i}$, so that the *total* coupling is the same independent of ϵ_i. To account for the possibility that the input channel to the second system may not match perfectly with an output channel from the first system, a *unitary mixer* m_1 is inserted between the physical inputs, and those corresponding to the required outputs. The same is done for the second system. The beam splitter e is necessary to account for the fact the light in the relevant output channel may not all be fed into the relevant input channel in the second system.

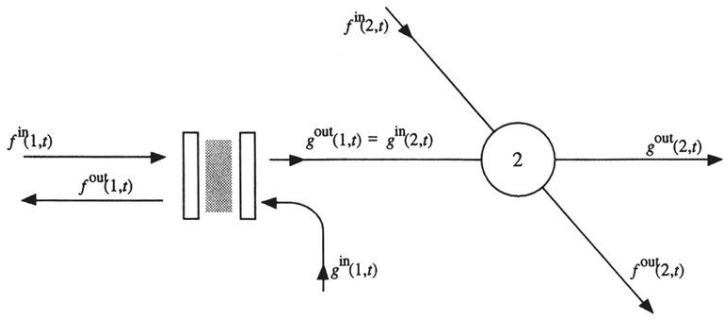

FIG. 3. Light from a two-sided harmonic oscillator coupled to a second system.